Active vibration control using compliant-based actuators

Sannia MARETA[1]; Dunant HALIM[1]; Atanas POPOV[2]

[1] Department of Mechanical, Materials and Manufacturing Engineering,

The University of Nottingham Ningbo China

[2] Department of Mechanical, Materials and Manufacturing Engineering,

The University of Nottingham, United Kingdom

ABSTRACT

In this work, an active vibration control method using compliant-based actuators is proposed for controlling a wide range of vibration and its noise-associated applications. The compliant-based actuator combines a conventional actuator with elastic elements, such as passive springs, that can be demonstrated to have better accuracy and robustness for force control compared to conventional stiff actuators. At high frequencies, the actuator behaves like a passive spring with low impedance, providing a better shock resistance to the actuator than the stiff actuator. These capabilities are beneficial for developing an effective vibration isolation system, particularly for controlling the vibration transmissibility at important low frequencies. The effect of compliant stiffness on the vibration control performance is investigated. It is shown that Proportional-Derivative (PD) control method using a compliant-based actuator can be used to obtain effective control of force transmissibility at low frequencies.

Keywords: Active Vibration Control, Compliant Actuators, Force Control
I-INCE Classification of Subjects Number(s): 46.4

1. INTRODUCTION

Vibration has an inhibiting effect on many precision industrial processes in addition to structures and transportation; such as for building and vehicle suspension system, hence the need for a means of cancelling this vibration. Various forms of vibration control strategies have been used over the years either passive (1), semi-active (2,3) or active (4); each with its own benefits and disadvantages.

Active vibration and noise control systems are usually made up of actuator drives (in the form of piezoelectric, pneumatic, etc.) connected to PID controllers (5). Nevertheless, the paper presents the use of compliant-based actuator with the aim of controlling vibration at low frequency.

Generally, compliant-based actuators can be defined as an actuation mechanism that allows the deviation from the actuator's equilibrium position, depending on the applied external force (6). The equilibrium position indicates the position of the actuator when the actuator generates zero force or zero torque. This actuator combines a conventional actuator with elastic elements, such as passive springs, which has the potential for active vibration control system. In fact, compliant-based actuators can be regarded as a novel actuator concept compared to the conventional 'stiff' actuators that are commonly used in robotic application, such as for walking robots (7), rehabilitation robots (8), exoskeletons (9) and medical applications (10). Industrial robots are normally operated using 'stiff' actuators to achieve precise position control for high repeatability, although it can cause a low performance for force control. Moreover, the 'stiff' actuators cannot counter well the external impacts and shocks caused by the environment (11). In contrast, these issues can be dealt better by using compliant actuators.

The first compliant-based actuator was developed by MIT Artificial Intelligence Laboratory (7,12), called the Series Elastic Actuator (SEA). SEAs are built from a combination of motors, linear springs,

[1] sannia.mareta@nottingham.edu.cn; dunant.halim@nottingham.edu.cn

[2] atanas.popov@nottingham.ac.uk

sensors and gear transmission (12). A number of other SEA designs have also been explored in (13,14). In contrast to ‘stiff’ actuators, where the actuator saturation leads to high torques at high load accelerations (such as the onset of a movement), the SEA takes on the natural impedance of the elasticity at high frequencies (7). Therefore, the more accurate and stable force control can be performed as the link rigidity is reduced.

This work considers the use of a compliant actuator for vibration control applications. The objective is to evaluate the behaviour of compliant actuator through the compliance analysis (Section 3) and force transmissibility analysis (Section 4). This aims to reduce the force transmission from the external disturbance to the ground, by using the compliant actuators that have been shown to have advantages for robotic actuation applications (15,16):

- Low output impedance, back-driveability and ability to store and release energy,
- Increasing the fidelity and stability of force control,
- Impact energy absorption to handle the external shock loads.

These properties are beneficial for developing an effective vibration isolation system, particularly for controlling vibration transmissibility at important low frequencies. However, the majority of previous works only focused on developing control to achieve accuracy and stability in robotic applications. Therefore, this paper aims to reveal a novel active vibration control mechanism using a compliant-based actuator. The performance of actuator with respect to its compliant stiffness is investigated, which assists in the selection of the actuator compliance.

2. DYNAMIC MODEL OF A COMPLIANT ACTUATOR

In this section, the dynamic model of a compliant actuator is developed as a basis for further analysis on vibration control. The actuator is based on a rotary actuator (motor) combined with a rack pinion system to achieve the linear actuation. The actuator generates motor torque T_m which is controlled by regulating the electrical current i that flows through the motor armature. A compliant actuator is constructed by adding a compliant element of stiffness k_c as shown in Figure 1. Here, J_{mp} is the overall rotational inertia of motor and pinion; x_1 is the linear displacement of the rack of mass M_p. The actuator applies a force f_l to the load of mass M_l, whose linear displacement is x_2. This is in contrast to the ‘stiff’ actuator where an infinite stiffness element is theoretically used. In contrast, this work investigates the use of the compliant actuator for active vibration control.

In this work, the mass-spring-damper configuration is used for the vibration control system as shown in Figure 2, where k_l and c_l are the spring stiffness and damping coefficient of the system, respectively. The control task is to minimize the force transmitted from the applied disturbance force f_d to the ground. The compliant actuator needs to be actively controlled to generate suitable control force f_l so to minimize the force transmissibility of the system.

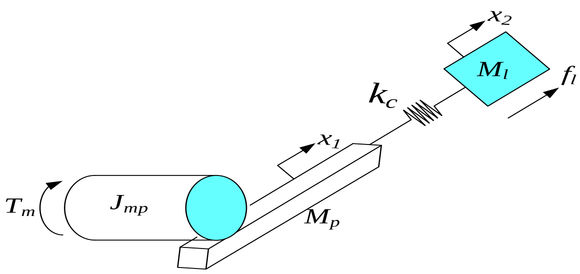

Figure 1 – The compliant actuator model with the rack pinion mechanism.

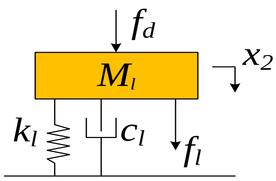

Figure 2 – The load mass with a spring-damper isolation system.

By considering the compliant actuator model, the motor torque is related to the electrical current by $T_m(t)=K_t i(t)$, where K_t is the motor torque constant and t is the time parameter. It is assumed that there is no viscous damping affecting the rotational motion of motor and pinion. The motion of the motor shaft can be derived both in time domain and Laplace domain, assuming zero initial conditions, as follows:

$$T_m(t) = K_t i(t) = J_{mp}\dot{\omega}(t) + T_p(t) \rightarrow T_m(s) = K_t I(s) = J_{mp} s\Omega(s) + T_p(s) \quad (1)$$

where ω is the shaft angular velocity, T_p is the torque of pinion, and $\Omega(s)$ is the Laplace transform of ω. By neglecting the backlash and other nonlinearities of the gear, the pinion torque $T_p(s)$ can be related the pinion force $F_p(s)$ and the radius of pinion r by:

$$T_p(s) = rF_p(s). \quad (2)$$

Moreover, the angular velocity of shaft and pinion, $\Omega(s)$, is related to the translational velocity of rack, $V(s)$. As $\theta(s)$ is the angle of motor shaft, then:

$$V(s) = r\Omega(s) = rs\theta(s), \quad (3)$$

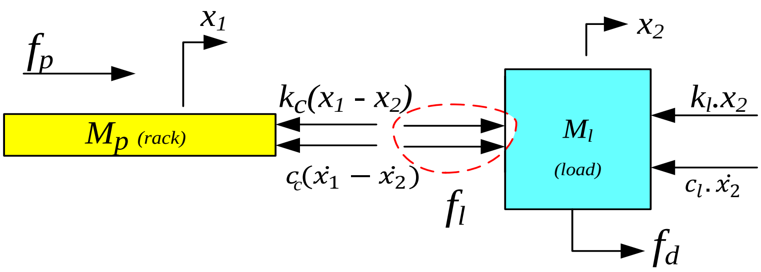

Figure 3 – Free body diagram of pinion's rack and load.

Figure 3 describes the free body diagram for the pinion's rack and load. The force transmitted from the pinion torque, $f_p(t)$, will cause the motion of rack as governed by:

$$f_p(t) = M_p\ddot{x}_1 + k_c(x_1 - x_2) + c_c(\dot{x}_1 - \dot{x}_2) \quad (4)$$

where k_c is the spring stiffness and c_c is the damping coefficient of compliant element. Here, c_c can be neglected as it is normally a very small value. On the other hands, the force $f_l(t)$ applied to the load mass via the compliant element is:

$$f_l(t) = k_c(x_1 - x_2) + c_c(\dot{x}_1 - \dot{x}_2). \quad (5)$$

Then, the motion of the load mass is affected by the disturbance force $f_d(t)$ and the load force $f_l(t)$:

$$f_d + k(x_1 - x_2) + c_c(\dot{x}_1 - \dot{x}_2) - k_l x_2 - c_l\dot{x}_2 = M_l\ddot{x}_2. \quad (6)$$

After the equations of motion for the compliant actuator are obtained, the analysis can be performed in the following Section.

3. COMPLIANCE ANALYSIS FOR VIBRATION CONTROL

Firstly, it is noted that the load force $F_l(s)$ is affected by the motor torque as shown in equation (7).

$$T_m(s) = J_{mp}s^2\theta(s) + rM_p s^2 X_1(s) + rF_l(s). \quad (7)$$

Since $\theta(s)=X_1(s)/r$, the displacement of pinion's rack $X_1(s)$ can be related to the load force $F_l(s)$ and the displacement of load mass $X_2(s)$, as:

$$F_l(s) = X_1(s)(c_c s + k_c) - X_2(s)(c_c s + k_c) \rightarrow X_1(s) = \frac{F_l(s) + X_2(s)(c_c s + k_c)}{(c_c s + k_c)}. \quad (8)$$

By substituting $X_1(s)$ from equation (8) to equation (7), the motor torque can be expressed as:

$$T_m(s)=\left(\frac{s^2\left(\frac{J_{mp}}{r}+rM_p\right)+rk_c+rsc_c}{sc_c+k_c}\right)F_l(s)+\left(s^2\left(\frac{J_{mp}}{r}+rM_p\right)\right)X_2(s). \tag{9}$$

Moreover, by considering the case where there is no load displacement, the transfer function from the motor torque to the load force becomes:

$$\frac{rF_l(s)}{T_m(s)}=\frac{sc_c+k_c}{s^2\left(\frac{J_{mp}}{r^2}+M_p\right)+sc_c+k_c}. \tag{10}$$

The above results show that the gain of the transfer function decreases at high frequencies, due to the existence of compliant element. If T_m is considered to be zero, the impedance $Z(s)$ can be obtained, which is the transfer function from the load displacement to the load force:

$$Z(s)=\frac{F_l(s)}{X_2(s)}=\frac{s^3c_c\left(\frac{J_{mp}}{r^2}+M_p\right)+s^2\left(\frac{J_{mp}}{r^2}+M_p\right)}{s^2\left(\frac{J_{mp}}{r^2}+M_p\right)+sc_c+k_c}. \tag{11}$$

For both transfer functions, there is a resonance that occurs at $\omega_2=\sqrt{\frac{rk_c}{H}}$ where H is defined as $\{(J_{mp}/r)+rM_p\}$. It can be seen that the actuator characteristics highly depends on the compliant stiffness, i.e. increasing the compliant stiffness will increase the resonance frequency. This will be investigated further in this work when the effect of load dynamics is considered in the modeling.

3.1 Comparison of Compliant Actuators and Conventional ‘Stiff’ Actuators

The effect of compliance on the actuator performance can be more clearly explained from the following frequency response $F_l(s)/X_1(s)$.

$$\frac{F_l(s)}{X_1(s)}=\frac{c_cM_ls^3+(k_cM_l+c_cc_l)s^2+(k_cc_l+c_ck_l)s+(k_ck_l)}{M_ls^2+(c_c+c_l)s+(k_c+k_l)}. \tag{12}$$

Since the compliant element generally has a very low damping, c_c can be assumed to be zero so $F_l(s)/X_1(s)$ can be simplified as:

$$\frac{F_l(s)}{X_1(s)}=k_c\frac{M_ls^2+c_ls+k_l}{\left(M_ls^2+c_ls+(k_c+k_l)\right)}. \tag{13}$$

It can be observed from the derived frequency response that there are anti-resonance and resonance characteristics, whose frequencies can be respectively estimated as $\omega_1=\sqrt{\frac{k_l}{M_l}}$ and $\omega_2=\sqrt{\frac{k_c+k_l}{M_l}}$. In this case, the anti-resonance occurs at a lower frequency than the resonance, $\omega_2>\omega_1$. It is important to look at the property of compliant actuator at higher frequencies, where the relationship between the rack’s displacement and load force can be simply expressed by the compliant stiffness k_c:

$$\frac{F_l(s)}{X_1(s)}\rightarrow k_c. \tag{14}$$

The results indicate the general benefit of the compliant actuator, since at higher frequencies, the position of rack is directly linked to the position of motor output shaft. Therefore, the error in the shaft position will not be translated into the large force error at the load. In other words, at high frequencies, the actuator behaves like a passive spring with low impedance. This is in contrast to the conventional ‘stiff’ actuator which a small error of the shaft will result in a larger force error of the load at high frequencies (17). Thus, for a particular vibration control application as being investigated in this work, such a compliant actuator will have benefits in achieving a more accurate force control for minimizing the force transmissibility of the vibration system.

In order to investigate the characteristics of the proposed compliant actuator for active vibration control application, the simulation model of the actuator is developed by using parameter values listed in Table 1.

Table 1 – Modelling parameters of the compliant-based actuator.

Definition	Symbol	Unit	Value
Moment of inertia for the motor and pinion	J_{mp}	kg.m^2	$1.90e^{-3}$
Radius of pinion	r	m	0.016
Mass of pinion's rack	M_p	kg	0.15
Damping coefficient for the compliant element	c_c	N.s/m	30
Stiffness of the compliant element	k_c	N/m	$4.8e^4$
Motor torque constant	K_t	N.m/A	5.80
Mass of load	M_l	kg	14.0
Stiffness of vibration isolation system	k_l	N/m	$4.8e^3$
Damping coefficient of vibration isolation system	c_l	N.s/m	9.0

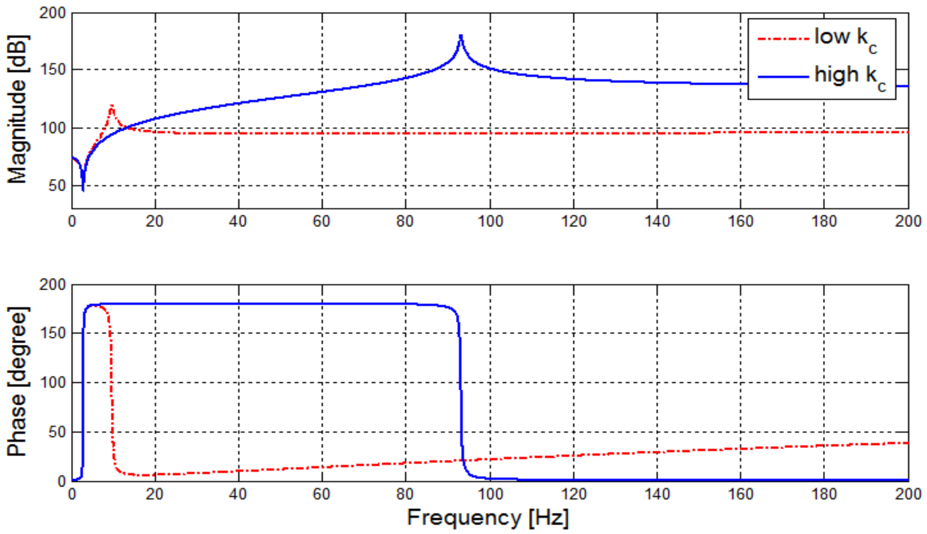

Figure 4 – Frequency response plot of $F_l(s)/X_1(s)$ for varying compliant stiffness k_c.

Figure 4 shows the frequency responses $F_l(s)/X_1(s)$ for the compliant actuators with two different values of compliant stiffness. The results indicate that the load force generally increases with the frequency for a given position of rack, X_1, or the position of motor output shaft. Similar to the case observed for the rotational compliant actuator (17), the effect of the position error for this linear motion can lead to a large load force error for the high compliant stiffness system, which is not desirable for high precision force control. This situation is important when a position-control based actuator, such as a servomotor is used, since a small position error can cause to a large force error.

In contrast, a compliant actuator with sufficiently low stiffness can avoid such a problem. Moreover, it can be seen from Figure 4 that the load force will be proportional to the position of the motor output shaft at higher frequencies. Thus, the load force applied to the load mass can be determined directly to the position of shaft by the compliant stiffness.

3.2 Effects of the Compliant Actuator to System Dynamics

In the previous discussion on the compliant actuator, the dynamics of the load mass is not considered. For the vibration control application, however, it is necessary to include the dynamics of the load mass as part of the whole system. It can be seen that changing the compliance stiffness will impact on the overall system dynamics since there are two inertia systems connected by compliances, i.e. a compliantly coupled system. Thus, the stiffness of compliant element will impact on the overall control performance. To investigate this, the relationship between the motor torque and the load force can be re-written as follows by including the load dynamics.

$$\frac{rF_l(s)}{T_m(s)} = \frac{rk_c\left(M_l s^2 + c_l s + k_l\right)}{HM_l s^4 + Hc_l s^3 + \left(H(k_c + k_l) + rk_c M_l\right)s^2 + rk_c c_l s + rk_c k_l}. \tag{15}$$

When a conventional ‘stiff’ actuator is used or $k_c \to \infty$, so the transfer function becomes:

$$\frac{rF_l(s)}{T_m(s)} = \frac{r\left(M_l s^2 + c_l s + k_l\right)}{(H + rM_l)s^2 + rc_l s + rk_l}. \tag{16}$$

Based on the transfer function, there are anti-resonance and resonance in the system, whose respective frequencies are $\omega_1 = \sqrt{\frac{k_l}{M_l}}$ and $\omega_2 = \sqrt{\frac{rk_l}{H + rM_l}}$.

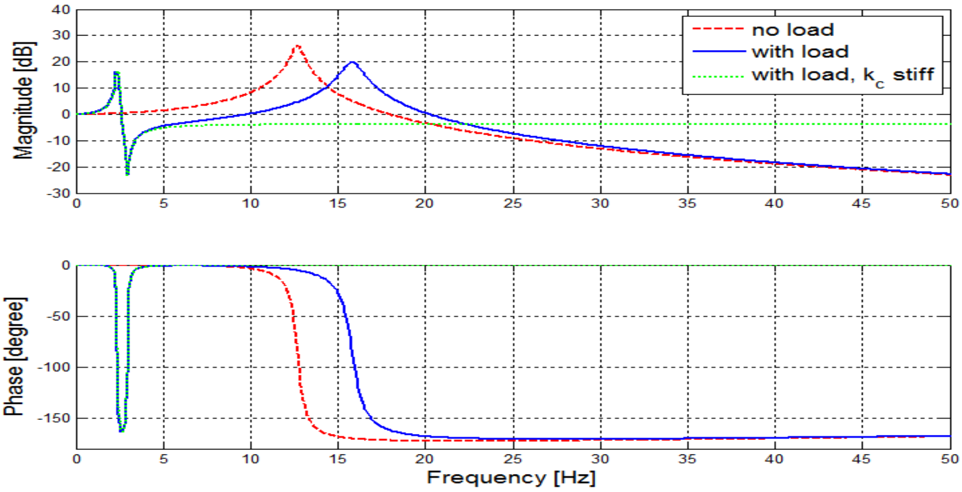

Figure 5 – Frequency responses $rF_l(s)/T_m(s)$ for different compliant actuator systems.

Frequency responses $rF_l(s)/T_m(s)$ are plotted in Figure 5 that compares two compliant actuator systems without and with load dynamics. For the system with load dynamics, anti-resonance occurs at lower frequency than the resonance frequency. In addition, two distinct frequency regions are also shown in Figure 5, a region below the anti-resonance frequency and another region above the resonance frequency.

At the lower frequency region, $rF_l(s)/T_m(s)$ has a unity gain with a zero phase difference, i.e. the motor torque is directly transmitted into the load force without any phase delay. However, at higher frequency region, the gain of $rF_l(s)/T_m(s)$ decreases below one with a non-zero phase difference, as the frequency increases. This can be expected because of the existence of compliant element used in the actuator. Although this reduces the operational bandwidth of actuator, the use of compliant element has the benefit of good external shock absorption (17), and this is an essential advantage for vibration control applications that can experience impulse-like excitations. On the other hands, as the stiffness of compliant element increases, the resonance frequency increases correspondingly which also increases the overall frequency bandwidth. In other words, there is a constant magnitude of the load force for a given motor torque. This behaviour can be seen for a ‘stiff’ actuator with a relatively high resonance frequency. Since the priority of active vibration control application is on low frequencies, it is reasonable to use the compliant actuator with a reduced operational bandwidth as a compromise for other benefits that such an actuator can offer.

4. CONTROL OF FORCE TRANSMISSIBILITY

4.1 Force Transmissibility

In developing an active vibration isolation system, one of the primary tasks is to minimize the force transmitted from an external disturbance to the ground. In this case, transfer function $F_t(s)/F_d(s)$ can be used to describe the force transmissibility of the system. It can be shown that $F_t(s)/F_d(s)$ is described by:

$$\frac{F_t(s)}{F_d(s)} = \frac{Hc_l s^3 + (Hk_l + rc_c c_l)s^2 + r(c_c k_l + k_c c_l)s + rk_c k_l}{\overline{D}(s)}, \tag{17}$$

$$\overline{D}(s) = HM_l s^4 + (H(c_c + c_l) + rc_c M_l)s^3 + (H(k_c + k_l) + rk_c M_l + rc_c c_l)s^2 + r(c_c k_l + k_c c_l)s + rk_c k_l \quad . \tag{18}$$

The system becomes a fourth order system due to the additional second order system contributed by the compliant actuator. The change of compliant stiffness will affect the overall force transmissibility so that a proper selection of the stiffness should be done to achieve a good vibration isolation performance, either in passive or active ways. The effect of changing the compliant stiffness can be observed in Figure 6. It is noted that the magnitude of force transmissibility decreases at higher frequencies, while the addition of second order system of actuator generating an additional weakly resonance in the system.

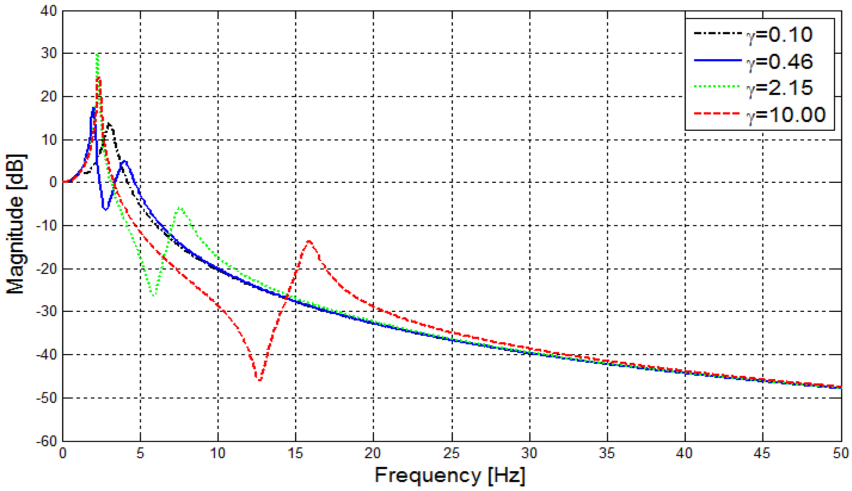

Figure 6 – Force transmissibility for a system using a compliant actuator: varying values of $\gamma = k_c / k_l$.

4.2 Active Control of Force Transmissibility

Various force control methods have been used with compliant-based actuators but they are mainly focused for robotic actuation applications (17-25). In this work, however, the focus will be on using the compliant actuator for active vibration control applications. In particular, how the transmitted force can be better controlled using a compliant actuator is observed. For this purpose, the effect of Proportional-Derivative (PD) controller on the force transmissibility is investigated, by considering the closed-loop system whose block diagrams are shown in Figure 7.

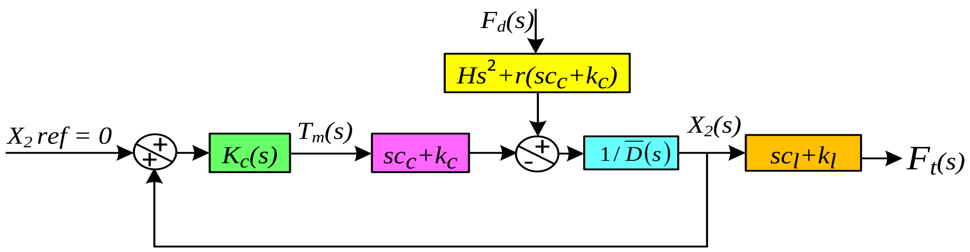

Figure 7 – The closed loop PD controller based on the position feedback.

In this system, a position sensor to measure the load displacement is used as the feedback sensor, and a PD controller used as $K_c(s)=K_p(1 + T_D s)$, where K_p and $K_p T_{D.}s$ represent the proportional control and derivative control terms, respectively.

Based on this closed-loop system configuration, the force transmissibility derivations have been done. For brevity, only the derivation results are shown here:

$$\frac{F_t(s)}{F_d(s)} = \frac{Hc_l s^3 + (Hk_l + rc_c c_l)s^2 + r(c_c k_l + k_c c_l)s + rk_c k_l}{\overline{D}(s) + K_c(s)(sc_c + k_c)}, \quad (19)$$

$$\overline{D}(s) + K_c(s)(sc_c + k_c) = HM_l s^4 + (H(c_c + c_l) + rc_c M_l)s^3 + \left(H(k_c + k_l) + rk_c M_l + rc_c c_l + K_p T_D c_c\right)s^2 \ldots$$
$$\cdots + \left(r(c_c k_l + k_c c_l) + K_p(T_D k_c + c_c)\right)s + k_c(rk_l + K_p). \quad (20)$$

If it is considered that c_c is very small, then the denominator of transfer function can be simplified to:

$$\overline{D}(s) + K_c(s)(sc_c + k_c) = HM_l s^4 + Hc_l s^3 + \left(H(k_c + k_l) + rk_c M_l\right)s^2 + k_c\left(rc_l + K_p T_D\right)s + k_c(rk_l + K_p). \quad (21)$$

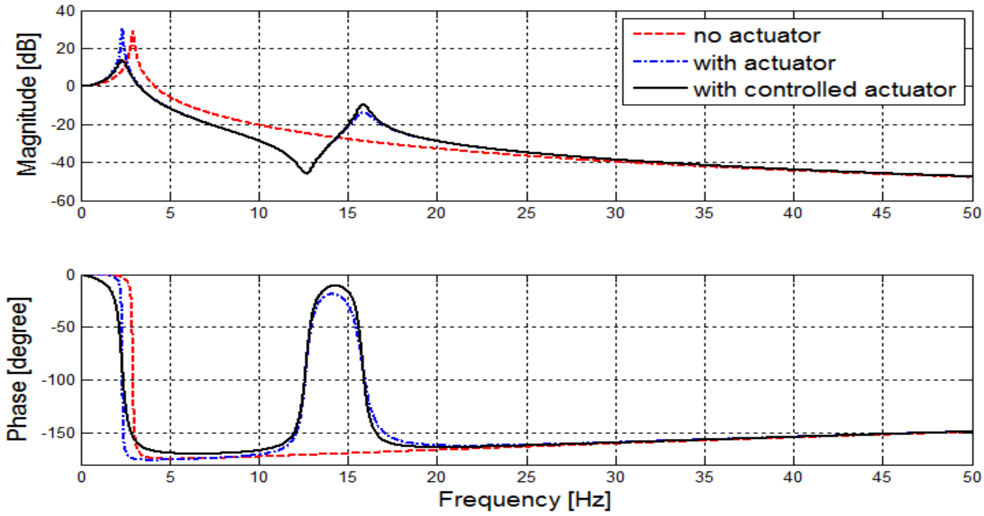

Figure 8 – Frequency response of $F_t(s)/F_d(s)$ with and without the active control system.

From equation (21), it can be observed that adding the proportional control K_p tends to increase the effective stiffness of the system, while the use of derivative control $K_p T_{D.}s$ tends to rise the effective damping of the system. The results can be seen in Figure 8 which shows the effect of derivative controller in reducing the dominant resonance peak of the force transmissibility by approximately 17 dB. Here, the effect of derivative control is more significant than adding the proportional control, particularly for reducing the resonance peak. There is a slight increase of transmissibility at the second resonance (16 Hz). However, it is considered to be a weak resonance, in contrast to the lower frequency dominant resonance.

5. CONCLUSIONS

The use of compliant-based actuator for active vibration control applications has been proposed in this work. The actuator consists of a rotary motor, linear spring and a set of rack and pinion. It is shown that the characteristics of the actuator highly depend on the compliant stiffness. An active control strategy using a PD controller is investigated for controlling the force transmissibility of a mass-spring-damper system. It is found that the proportional control term can increase the effective stiffness of the system, while the derivative control terms can increase the effective damping.

For vibration control, the dynamics of the load mass as part of the whole system and low frequency range are shown to be important to be considered. The compliant-based actuator can be used to actively control the force transmission, as demonstrated by 17 dB of force transmissibility reduction at the dominant resonance based on simulations. Therefore, by considering the observed benefits of the compliant actuators, it is demonstrated that they have good potential to be used for active vibration control applications.

ACKNOWLEDGEMENTS

The authors wish to acknowledge the support provided by Ningbo Science and Technology Bureau – Technology Innovation Team (2011B81006), China.

REFERENCES

1. Reitherman R. Earthquakes and Engineers: An International History. Reston, VA: ASCE Press; 2012. ISBN 9780784410714.
2. Karnopp D, Crosby MJ, Harwood RA. Vibration control using semi-active force generators. ASME Journal of Engineering for Industry, 1974; 96(2): pp.619–626.
3. Choi SB, Seong MS, Kim KS. Vibration Control of an Electrorheological Fluid-Based Suspension System with an Energy Regenerative Mechanism. Journal of Automobile Engineering, 2009; 223: 459-469.
4. Halim D, Barrault G, Cazzolato B. Active control experiments on a panel structure using a spatially-weighted objective method with multiple sensors. Journal of Sound and Vibration, 2008; vol. 315:1-21
5. Hansen C, Snyder S, Qiu X, Brooks L, Moreau D. Active Control of Noise and Vibration, Second Edition, CRC Press; 2012; 1553 Pages.
6. Van Ham R, Sugar TG, Vanderborght B, Hollander KW, Lefeber D. Compliant Actuators Design, IEEE Robotics & Automation Magazine; 2009.
7. Robinson DW, Pratt JE, Paluska DJ, Pratt GA. Series elastic actuator development for a biomimetic walking robot. In IEEE/ASME International Conference on Advanced Intelligent Mechatronics, 1999.
8. Zhu C, Oda M, Yu H, Watanabe H, Yan Y. Walking support and power assistance of a wheelchair typed omnidirectional mobile robot with admittance control mobile robots – current trends. In Zoran Gacovski (Ed.); 2011. ISBN: 978-953-307-716-1, InTech.
9. Van der Kooij H, Veneman JF, Ekkelenkamp R. Compliant Actuation of Exoskeletons, Mobile Robots: towards New Applications. Aleksandar Lazinica (Ed.); 2006. ISBN: 978-3-86611-314-5.
10. Nef T, Mihelj M, Colombo G, Riener R. ARMin-robot for rehabilitation of the upper extremities. In Proc. of IEEE International Conference on Robotics and Automation, 2006; pp. 3152–3157.
11. Yu H, Huang S, Chen G, Toh SL, Cruz MSTA, Ghorbel Y, Zhu C. Design and analysis of a novel compact compliant actuator with variable impedance. In Proc. IEEE Int. Conf. Robotics and Biomimetics (ROBIO), 2012; pp. 1188-1193.
12. Pratt G, Williamson M. Series elastic actuators. In Proc. of IEEE/RSJ International Conference on Intelligent Robots and Systems, 1995; Vol. 1, pp. 399--406.
13. Torres-Jara E, Banks J. A simple and scalable force actuator. In Proceedings of 35th International Symposium on Robotics, Paris, France 2004.
14. Sensinger JW, Weir R. Improvements to series elastic actuators. In Proceedings of the 2nd IEEE/ASME International Conference on Mechatronic and Embedded Systems and Applications, 2006; p.1–7.
15. Pratt JE, Krupp BT. Series elastic actuators for legged robots. In Proc. SPIE 5422, Unmanned Ground Vehicle Technology VI, 2004; pp. 135–144.
16. Pratt JE, Krupp BT, Morse C. Series elastic actuators for high fidelity force control. Industrial Robot Journal, 2002; Vol. 29, No. 3, pp. 234-241.
17. Williamson, M. Series Elastic Actuators. Master Thesis, Electrical Engineering and Computer Science Department, Massachusetts Institute of Technology; 1995.
18. Vallery H, Ekkelenkamp R, Van der Kooij H, Buss M. Passive and Accurate Torque Control of Series Elastic Actuators. IEEE/RSJ International Conference, IROS, 2007; p.3534-3538.
19. Whitney DE. Force Feedback Control of Manipulator Fine Motions. Trans ASME Journal of Dynamic Systems, Measurement and Control 1977; 99:pp. 91-97.
20. Hogan N. Impedance Control: An approach to manipulation: Part 1 – theory, Part 2 - Implementation, and Part 3 – Applications. ASME J. of Dynamic Systems, Measurement and Control, 1985; 107: 1-24.
21. Sugano S, Tsuto S, Kato I. Force control of the robot finger joint equipped with mechanical

compliance adjuster. In Proceedings of IEEE/RSJ International Conference on Intelligent Robots and Systems, Raleigh, NC, 1992; p. 2005–13.
22. Tasch ADU. A two-dof manipulator with adjustable compliance capabilities and comparison with the human finger. J. Robotic System, 1996; 13(1):25–34.
23. Misgeld BJE, Gerlach-Hahn K, R¨uschen D, Pomprapa A, Leonhardt S. Control of adjustable compliant actuators. Journal of Machines 2014; 2:p.134-157.
24. Qiao T, Bi S. Cascaded control of compliant actuators in friendly robotics. U.P.B. Sci. Bull., Series D, 2013; Vol. 75, Iss. 1.
25. Sugar TG. A novel selective compliant actuator. Journal of Mechatronics, 2002; 12:p.1157–1171.